

Copper(II) metal-organic networks derived from bis(pyridylformyl)piperazine ligands and aromatic polycarboxylates: 2-D layered structures and a novel 3,5-connected binodal 3-D topology

Xiu-Li Wang^{*}, Hong-Yan Lin, Bao Mu, Ai-Xiang Tian and Guo-Cheng Liu

^a Faculty of Chemistry and Chemical Engineering, Bohai University, Jinzhou, 121000, P.R. China

ELECTRONIC SUPPLEMENTARY INFORMATION

Table S1. Selected Bond Distances (Å) and Angles (deg) for Compounds 1-3

Compound 1			
Cu(1)–O(1)	1.937(3)	Cu(1)–O(5)	2.305(3)
Cu(1)–O(3)	1.953(3)	Cu(1)–N(1)#1	2.022(4)
Cu(1)–O(1W)	1.978(3)		
O(1)–Cu(1)–O(3)	177.26(12)	O(1)–Cu(1)–O(1W)	88.74(12)
O(3)–Cu(1)–O(1W)	89.75(12)	O(1)–Cu(1)–N(1)#1	90.12(13)
O(3)–Cu(1)–N(1)#1	91.93(13)	O(1W)–Cu(1)–N(1)#1	165.17(13)
O(1)–Cu(1)–O(5)	89.65(12)	O(3)–Cu(1)–O(5)	88.17(12)
O(1W)–Cu(1)–O(5)	93.68(12)	N(1)#1–Cu(1)–O(5)	101.10(13)
Symmetry code: #1– x + 1/2, – y + 1, z + 1/2.			
Compound 2			
Cu(1)–N(1)	2.019(4)	Cu(1)–O(4)#1	1.940(3)
Cu(1)–O(1)	1.947(3)	Cu(1)–N(4)#2	1.998(4)
Cu(1)–O(5)#3	2.291(3)		
O(4)#1–Cu(1)–O(1)	165.57(14)	O(4)#1–Cu(1)–O(5)#3	108.45(13)
O(4)#1–Cu(1)–N(4)#	87.65(16)	O(1)–Cu(1)–O(5)#3	85.98(13)
O(1)–Cu(1)–N(4)#2	91.45(16)	N(4)#2–Cu(1)–O(5)#3	93.55(16)
O(4)#1–Cu(1)–N(1)	91.12(15)	N(1)–Cu(1)–O(5)#3	92.14(15)
O(1)–Cu(1)–N(1)	88.34(15)	N(4)#2–Cu(1)–N(1)	174.27(16)
Symmetry code: #1 – x + 3/2, y + 1/2, – z + 3/2; #2 x, y, z – 1; #3 – x + 1, – y, – z + 2.			

Compound 3			
Cu(1)–O(4)	1.934(2)	Cu(1)–N(1)	2.018(3)
Cu(1)–O(1)	1.945(2)	Cu(1)–O(7)	2.390(3)
Cu(1)–O(1W)	1.962(2)		
O(4)–Cu(1)–O(1)	176.06(10)	O(1W)–Cu(1)–N(1)	174.82(10)
O(4)–Cu(1)–O(1W)	90.88(9)	O(4)–Cu(1)–O(7)	88.63(10)
O(1)–Cu(1)–O(1W)	86.21(9)	O(1)–Cu(1)–O(7)	93.97(10)
O(4)–Cu(1)–N(1)#1	91.76(10)	O(1W)–Cu(1)–O(7)	89.05(9)
O(1)–Cu(1)–N(1)#1	91.36(10)	N(1)#1–Cu(1)–O(7)	86.56(10)
Symmetry code: #1 $-x, y, -z$.			

Table S2. Hydrogen–Bonding Geometry (Å, °) for Compounds 1–3

D–H···A	D–H	H···A	D···A	<D–H···A
Compound 1				
O(1W)–H(1A)···O(4) ^a	0.82	1.87	2.679(4)	168
O(1W)–H(2B)···O(2) ^a	0.82	1.86	2.659(4)	166
O(2W)–H(2A)···O(3)	0.82	2.19	2.983(5)	163
O(3W)–H(3A)···O(2) ^b	0.82	2.20	2.883(6)	141
Compound 2				
O(6)–H(6)···O(3) ^a	0.82	1.69	2.494(5)	166
O(1W)–H(1A)···O(2)	0.82	2.00	2.815(10)	170
O(1W)–H(1B)···O(7) ^b	0.82	2.22	3.031(12)	170
Compound 3				
O(1W)–H(1A)···O(2) ^a	0.82	1.85	2.655(3)	167
O(1W)–H(1B)···O(5) ^a	0.82	1.88	2.692(3)	172
Symmetry code for 1: (a) $-x, -y + 1, -z + 2$; (b) $-x + 1/2, -y + 1, z - 1/2$; for 2: (a) $x - 1/2, -y - 1/2, z + 1/2$; (b) $-x + 2, -y, -z + 2$; for 3: (a) $-x + 1/2, -y + 1/2, -z + 1$.				

Fig. S1. (a) The 2-D grid layer structure formed by **3-bpfp** and BDC ligands in **1** (A: $x, 1/2 - y, z$; B: $-1/2 - x, 1/2 + y, -1/2 + z$; C: $-1/2 - x, -y, -1/2 + z$; D: $-1/2 - x, -1/2 + y, -1/2 + z$; E: $-1/2 - x, -1 - y, -1/2 + z$; F: $-1/2 - x, 1 - y, -1/2 + z$; G: $-1/2 - x, 3/2 + y, -1/2 + z$); (b) The undulated 1-D polymer chain formed by BDC ligands in **1** (B: $-1/2 - x, 1/2 + y, -1/2 + z$; C: $-1/2 - x, -y, -1/2 + z$; D: $-1/2 - x, -1/2 + y, -1/2 + z$; E: $-1/2 - x, -1 - y, -1/2 + z$; F: $-1/2 - x, 1 - y, -1/2 + z$; G: $-1/2 - x, 3/2 + y, -1/2 + z$); (c) The 2-D layer structure of **1** formed by BDC and **3-bpfp** ligands along *c*-axis in **1**. (H atoms are omitted for clarity).

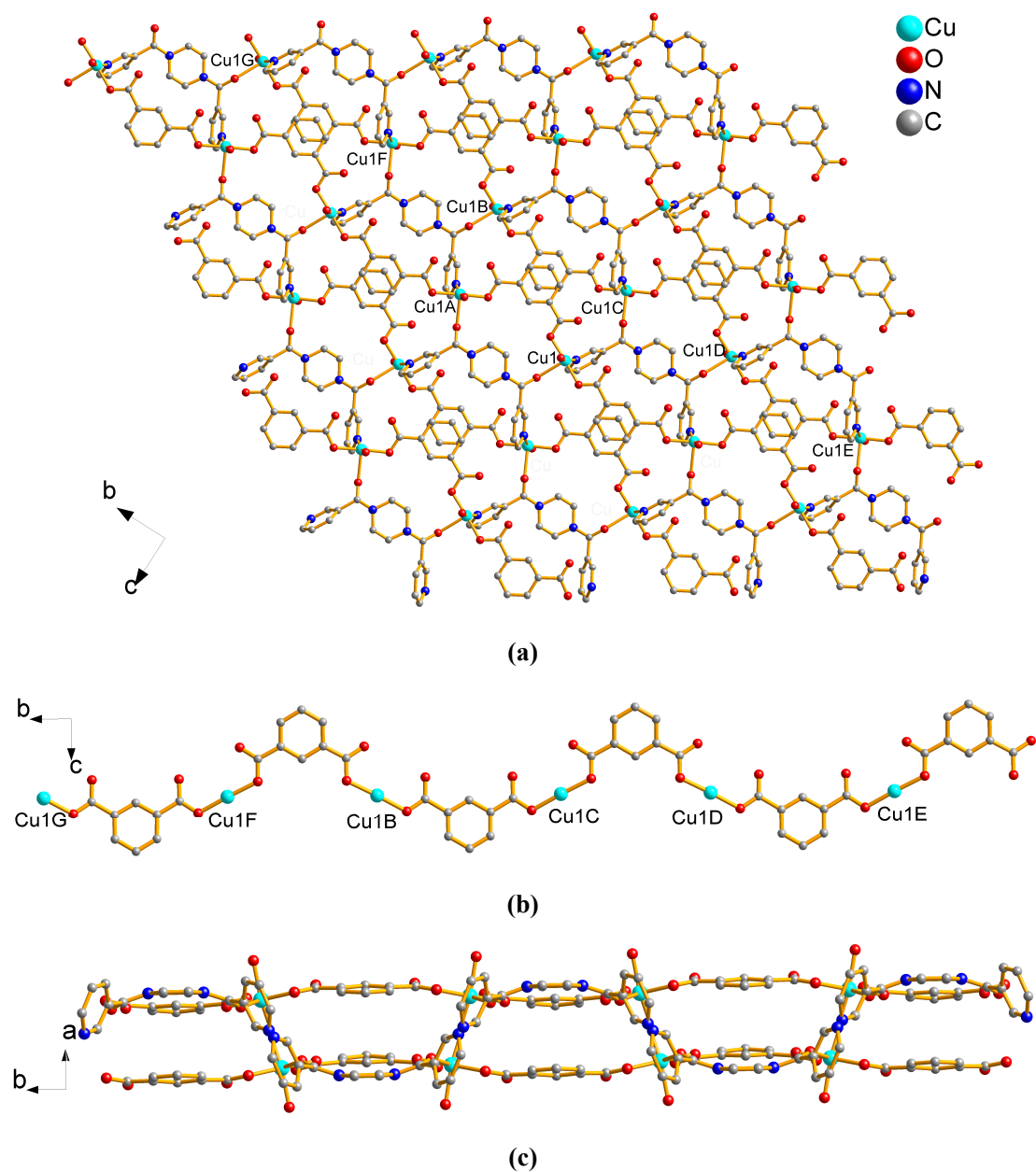


Fig. S2. (a) The 3-D packing structure of **1** without lattice water molecules; (b) The 3-D packing structure of **1** containing lattice water molecules. (part of the H atoms are omitted for clarity)

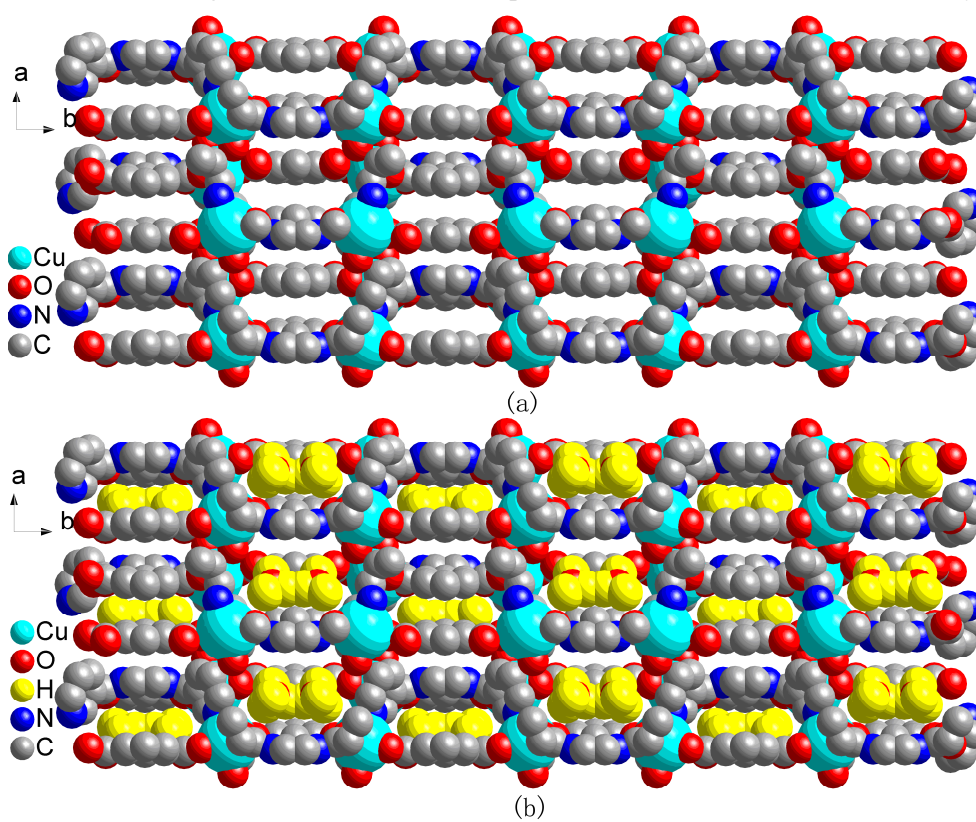


Fig. S3. (a) The 3-D packing structure of **2** without lattice water molecules; (b) The 3-D packing structure of **2** containing lattice water molecules. (part of the H atoms are omitted for clarity)

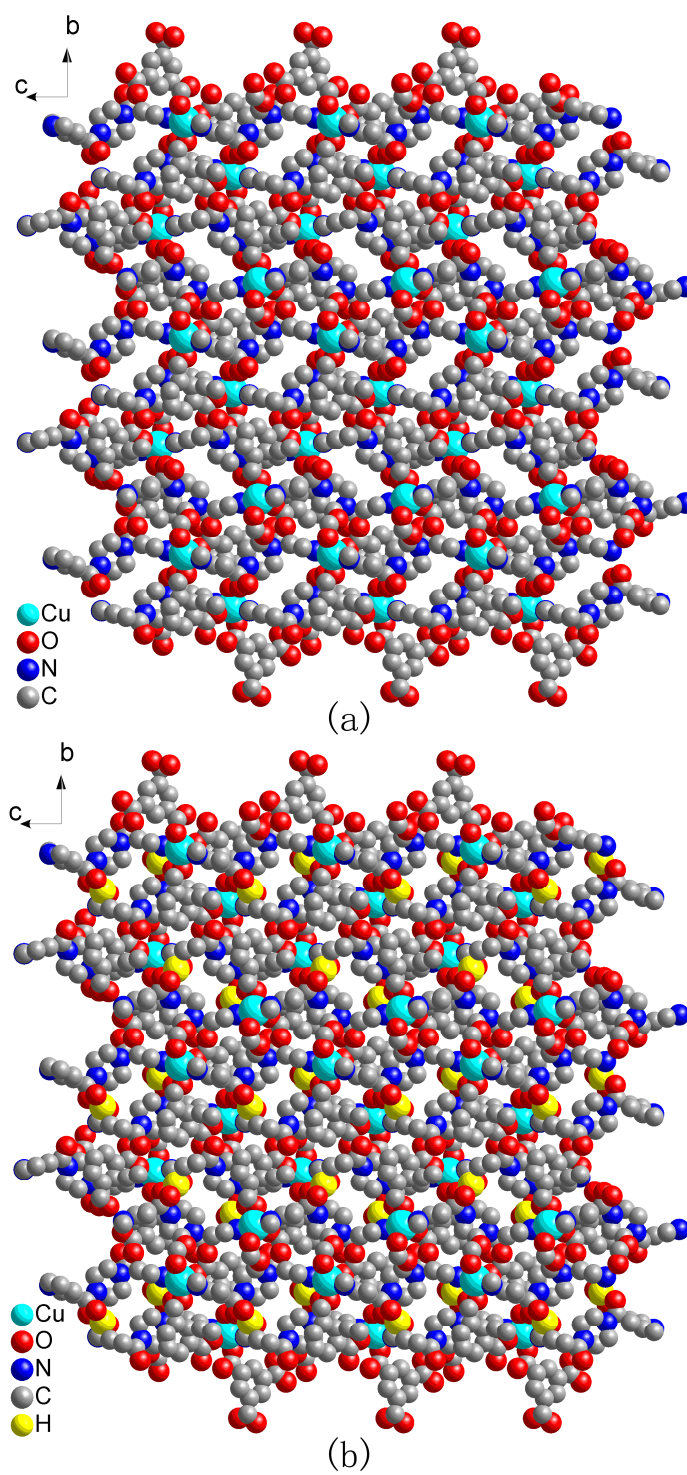


Fig. S4. (a) The 2-D undulating network of **3**; (b) The 2-D layer network of **3**. (H atoms are omitted for clarity).

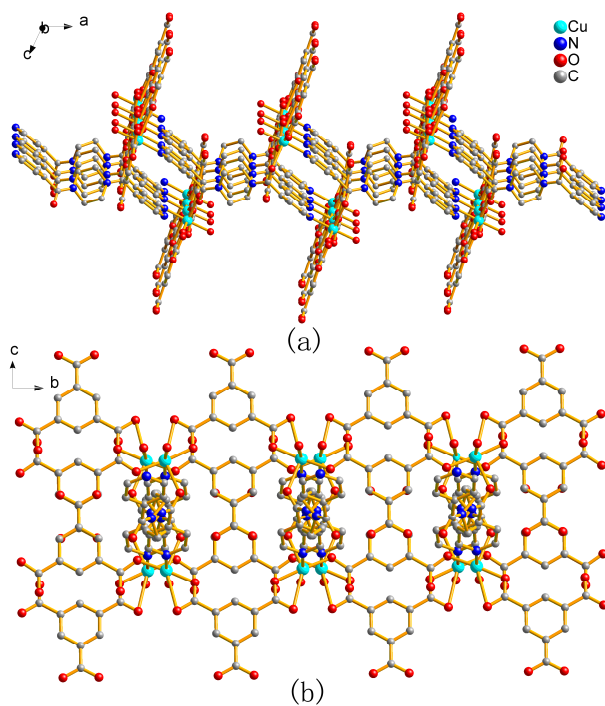


Fig. S5. (a) The 3-D stacking structure with large voids in **3**. (H atoms are omitted for clarity)

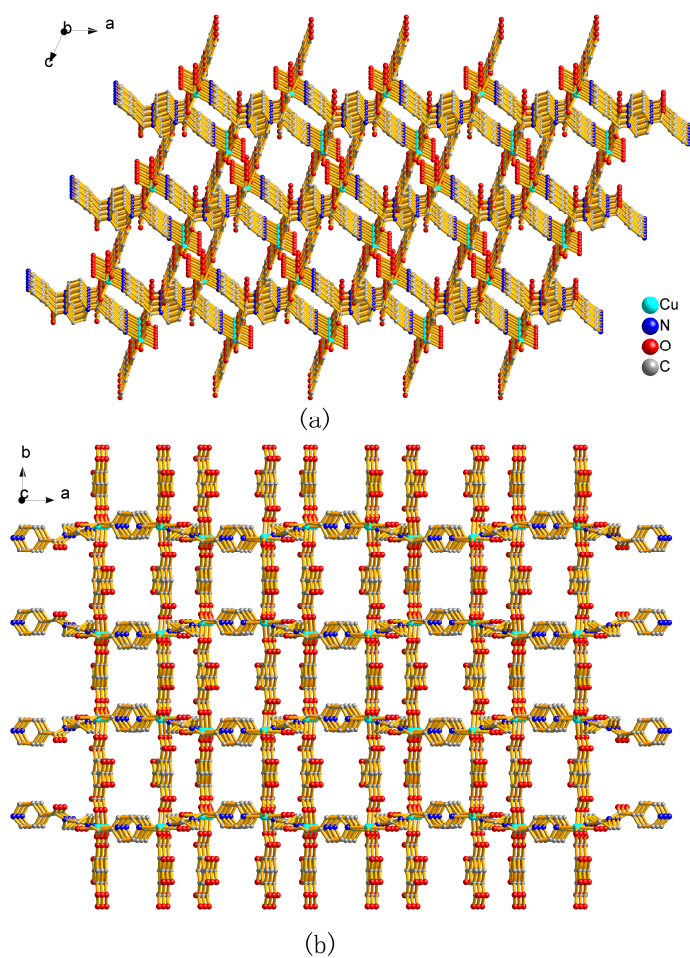
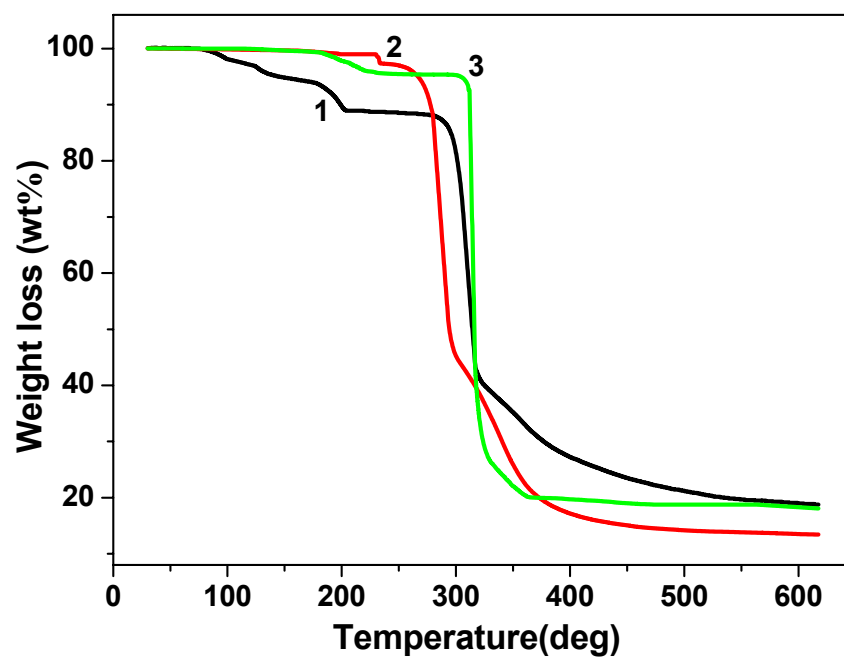


Fig. S6 TG curves for compounds 1-3.



Preparation of compounds 1-3 modified CPEs

The modified 1-CPE was fabricated as follows: 0.35 g graphite powder and 0.02 g compound 1 were mixed and ground together by agate mortar and pestle for approximately 30 min to achieve an even, dry mixture; to the mixture 0.14 ml paraffin oil was added and stirred with a glass rod; then the homogenized mixture was used to pack 3 mm inner diameter glass tubes to a length of 0.5 cm. The electrical contact was established with the copper stick, and the surface of the modified CPE was wiped with weighing paper. The same procedure was used for preparation of 2-CPE, 3-CPE, and the bare CPE without copper compounds.

Fig. S7 Cyclic voltammograms of 1-CPE in 1M H₂SO₄ solution at different scan rates (from inner to outer) 20, 40, 60, 80, 100, 120, 140, 160 and 180 mV s⁻¹ of 1-CPE. The inset shows the plots of the anodic and the cathodic peak currents vs. scan rates.

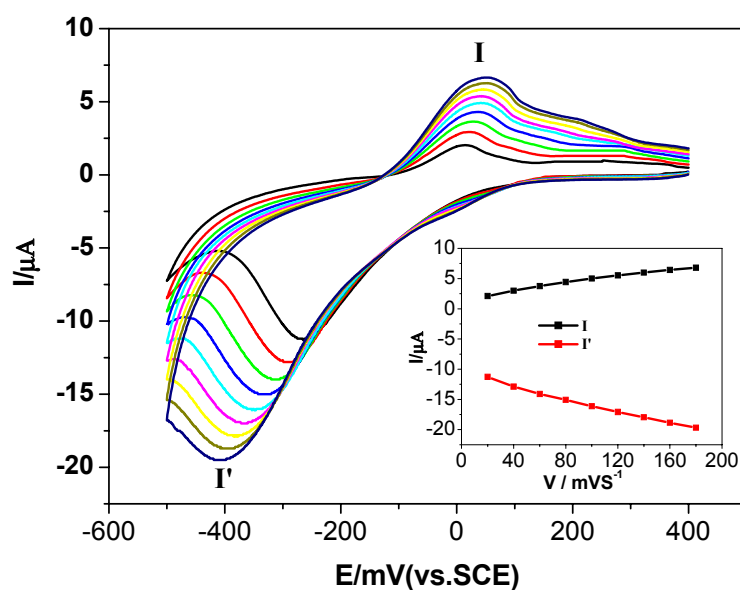


Fig. S8. The IR spectrum of compound 1.

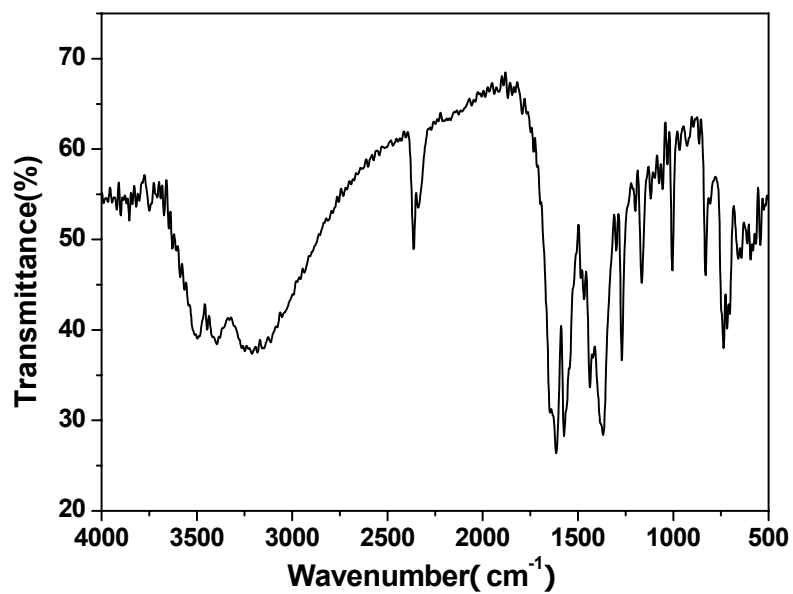


Fig. S9. The IR spectrum of compound 2.

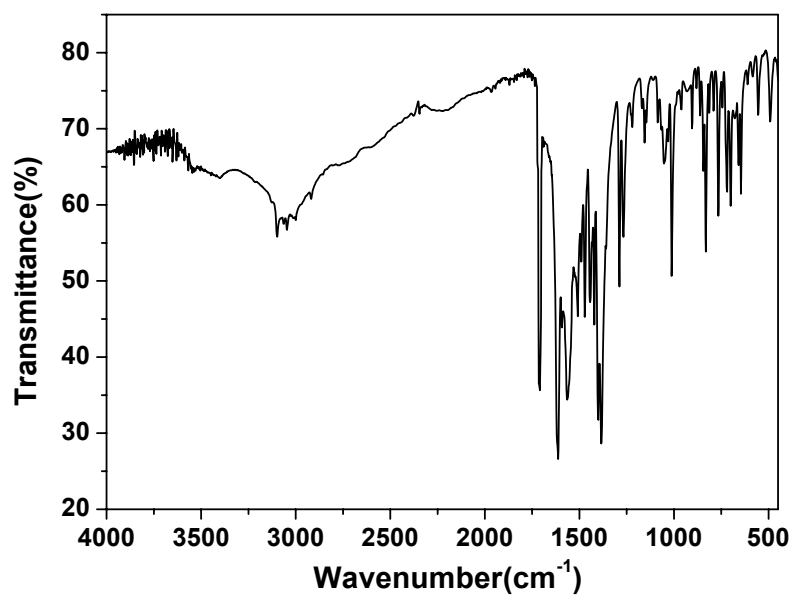
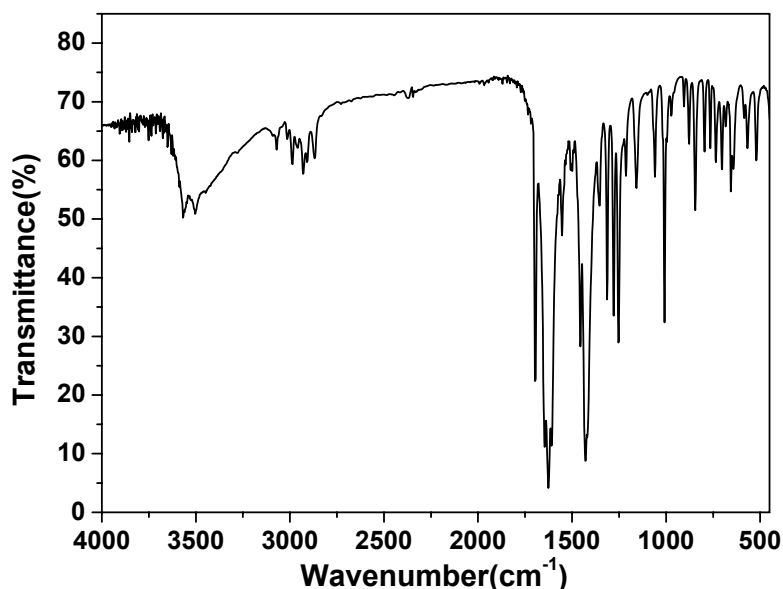


Fig. S10. The IR spectrum of compound 3.



Infrared Spectra

The main features in the IR spectra of compounds **1–3** concern the carboxylate groups and the ligand **3-bpfp** or **4-bpfp** (Fig. S8–10, Supporting Information). For these four compounds, the typical stretching bands of carboxylate groups were mainly displayed between 1300 and 1650 cm^{-1} . The bands at about 1550, 1420, 1010, and 720 cm^{-1} may be attributed to the $\nu_{\text{C-N}}$ stretching of the pyridyl ring or piperazinyl ring. In compound **1**, no strong absorption peaks around 1700 cm^{-1} for $-\text{COOH}$ are observed, indicating that carboxyl groups of organic moieties in **1** are completely deprotonated¹; while the IR spectra of **2** and **3** display strong absorption peaks at 1708 and 1697 cm^{-1} , respectively, indicating the presence of carboxyl groups coming from HBTC anions. Weak absorptions observed at 2860–3050 cm^{-1} can be attributed to the $\nu_{\text{C-H}}$ of the pyridyl group. The strong broad band at around 3500 cm^{-1} is assigned to the vibrations of hydroxyl groups.

- 1 (a) X .J. Gu, D. F. Xue, *Cryst. Growth Des.*, 2006, **6**, 2551; (b) L. J. Bellamy, *The Infrared Spectra of Complex Molecules*; Wiley, New York, 1958; (c) C. P. Li, Q. Yu, J. Chen and M. Du, *Cryst. Growth Des.*, 2010, **10**, 1623.

Fig. S11 XRD patterns: (a) simulated from single-crystal X-ray data; (b) as-synthesized compound 1.

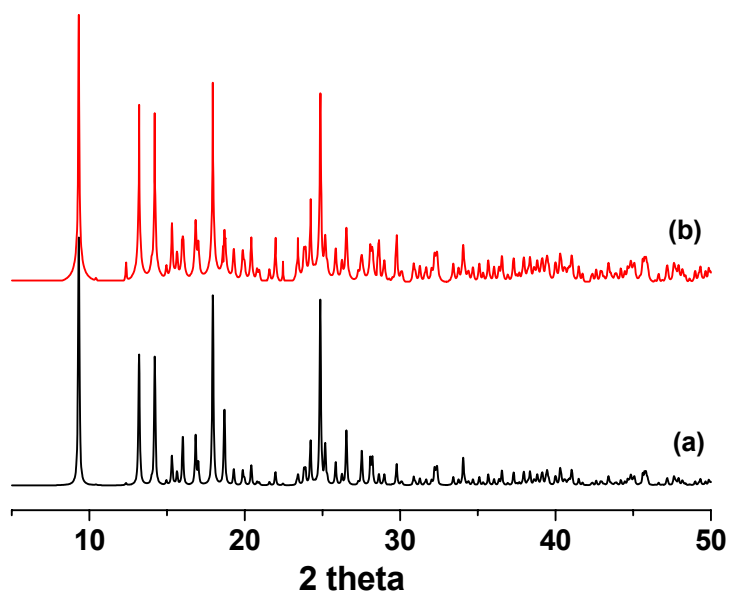


Fig. S12 XRD patterns: (a) simulated from single-crystal X-ray data; (b) as-synthesized compound 2.

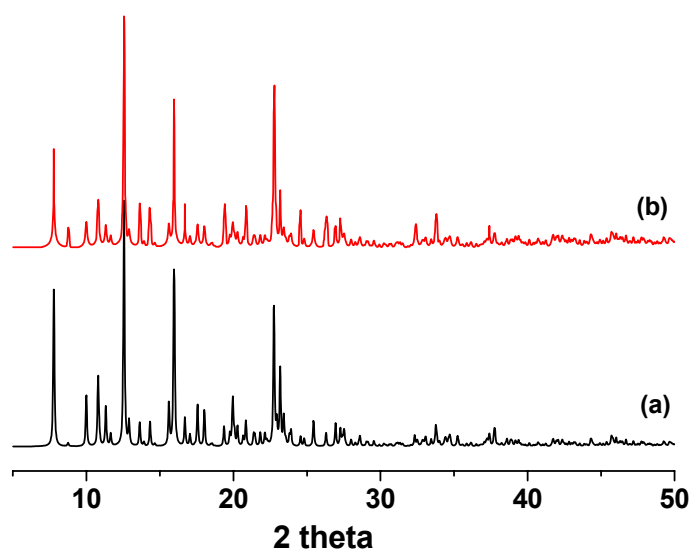
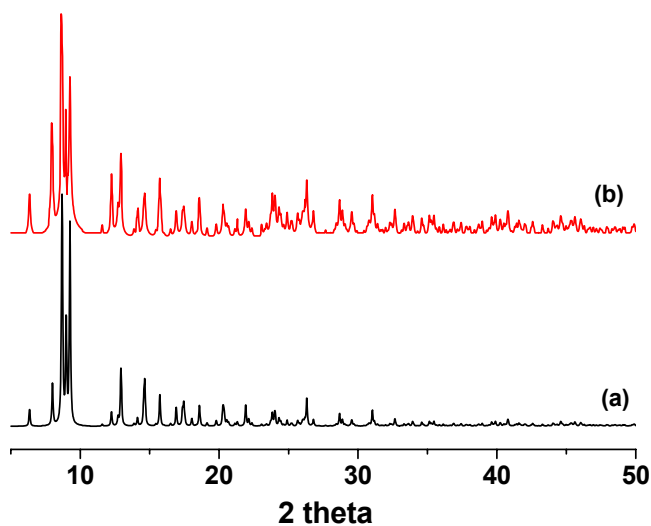


Fig. S13 XRD patterns: (a) simulated from single-crystal X-ray data; (b) as-synthesized compound **3**.



Powder X-ray diffraction

The XRD spectra for compounds **1-3** are included in the Supporting Information (**Fig. S11-13**). The powder X-ray diffraction patterns of as-synthesized crystals of **1-3** were almost identical to that calculated from the single-crystal structures. The diffraction peaks of the simulated and experimental patterns match well in key positions, indicating the phase purities of compounds **1-3**.